

ELECTRO-CHEMO-MECHANICAL SIMULATION OF 3D-MICROSTRUCTURES FOR LITHIUM-ION BATTERIES

Tobias Hofmann^{1*}, Daniel Westhoff², Julian Feinauer², Heiko Andrä¹, Jochen Zausch¹, Volker Schmidt², Ralf Müller³

¹ Material and Flow Simulation, Fraunhofer Institute of Industrial Mathematics ITWM, Kaiserslautern, Germany, tobias.hofmann@itwm.fraunhofer.de

² Institute of Stochastics, Ulm University, Germany

³ Chair of Applied Mechanics, University of Kaiserslautern, Germany

Key words: multiphysics, electrochemistry, batteries, elasticity, stochastic microstructure modeling

Abstract. A micromodel coupling lithium-ion diffusion and electric potentials to a linear elasto-plastic model is applied. The resulting problem is discretized on a regular voxel grid with a finite-volume method and solved by an adaptive iterative scheme. The algorithm does not require the assembly of a Jacobian and applies the immersed interface method for the electrochemical problem. An established elastic solver optimized for non-linear heterogeneous structures is generalized to describe mechanical strains resulting from lithium-ion intercalation. Numerical examples on several structures are given, including academic structures and microstructures given by computer tomography compared to microstructures drawn from stochastic microstructure models. It is found that the structures drawn from the calibrated model resemble the mechanical properties of the structures gained by tomographic imaging, which serves as an additional validation of the stochastic microstructure modeling approach.

Introduction

Some electrode materials in lithium-ion batteries show deformation and degradation during operation. The imbalanced intercalation of the lithium ions into the lattice structure of active particles causes concentration gradients. The stresses resulting from these gradients can damage and destroy the battery cell. Computer simulations of these stresses during charging and discharging can help to understand this process and support the development of more efficient battery cell structures.

A micromodel coupling lithium-ion diffusion to the electric potential and Butler-Volmer interface currents and linear elasticity is applied [4, 9]. This enables the resolution of a complex three-dimensional porous microstructure of the anode and cathode material in the liquid electrolyte. Additionally mechanical stresses resulting from strains depending

on the local concentration of lithium ions are computed [1, 15]. This results in a system of partial differential equations. For the numerical solution, a finite volume method is applied for the discretization in space, while the time discretization is realized by an implicit Euler method. A domain decomposition algorithm based on the immersed interface method [10] is extended for the diffusion and Poisson equation. By this, large, adaptive time steps are possible in arbitrary complex domains [5].

Numerical examples are given to demonstrate the coupling effects between the electrochemical model and the mechanical model. First, the method is applied to a single spherical anode particle. Moreover, computer tomography data is used to develop stochastic 3D models for microstructure generation [2, 8, 14]. The electrochemical solution on these microstructures has been validated recently [3], and a good agreement of spatially resolved electrochemical properties was found between tomographic image data and realizations of the calibrated model. In the present paper, for an additional validation of the stochastic modeling approach, mechanical properties are compared using the method described above. The spatial distribution of stress invariants along the thickness direction is calculated, and a good match between the results for tomographic image data and corresponding model realizations is found.

1 Electro-chemo-mechanical model

A cuboid domain $\Omega = (0, L_1) \times (0, L_2) \times (0, L_3) \subset \mathbb{R}^3$ denotes the microstructure of a battery cell and consists of the two solid electrodes, anode Ω_a and cathode Ω_c , and the liquid electrolyte Ω_e . A time-dependent problem is posed on the domain $T = (0, t_0)$. For concentration, electric potential and displacement, partial differential equations are given on each of the three domains: anode, cathode and electrolyte.

Electro-chemical model

Transport equations in the electrolyte domain, the anode domain, and the cathode domain are introduced separately based on [9]. The transport equations for ion concentration c_e and the electric potential ϕ_e in a liquid electrolyte are considered as

$$\begin{aligned} \partial_t c_e &= \nabla \cdot \left[\left(\frac{D_e}{RT} + \frac{\kappa_e t_+ (t_+ - 1)}{F^2 c_e} \right) \nabla c_e + \frac{\kappa_e t_+}{F} \nabla \phi_e \right], \\ 0 &= \nabla \cdot \left[\kappa_e \frac{(t_+ - 1)}{F c_e} \nabla c_e + \kappa_e \nabla \phi_e \right]. \end{aligned} \tag{1}$$

Here constants R , T and F are the universal gas constant, the temperature, and the Faraday constant, respectively. The electro-chemical properties of the electrolyte are given by its diffusivity D_e and its conductivity κ_e . Depending on the transference number t_+ , the transport of positive lithium ions is coupled to the transport of additional negative anions. Inside the electrode material, the lithium ion diffusion c_s and the electric potential

ϕ_s are decoupled by the equations

$$\begin{aligned}\partial_t c_s &= \nabla \cdot \left[\frac{D_s}{RT} \nabla c_s \right], \\ 0 &= \nabla \cdot [\kappa_s \nabla \phi_s],\end{aligned}\tag{2}$$

where D_s denotes the corresponding diffusivity, and κ_s the conductivity.

Elasto-plastic model

The stress-strain relationship model presented in this work is based on a linear-elastic model, see [1] and [15]. The strain $\boldsymbol{\varepsilon}$ in the solid is modified to include a chemical part

$$\boldsymbol{\varepsilon} = \boldsymbol{\varepsilon}_{\text{el}} + \boldsymbol{\varepsilon}_{\text{ch}} + \boldsymbol{\varepsilon}_{\text{pl}},\tag{3}$$

and consists therefore of an elastic part $\boldsymbol{\varepsilon}_{\text{el}}$, a chemical part $\boldsymbol{\varepsilon}_{\text{ch}}$ and a plastic part $\boldsymbol{\varepsilon}_{\text{pl}}$. The constitutive relationships for the displacement u , the elastic strain $\boldsymbol{\varepsilon}_{\text{el}}$, and the stress $\boldsymbol{\sigma}$ are then given as

$$\begin{aligned}\boldsymbol{\varepsilon}_{\text{el}} &= \frac{1}{2}(\nabla \vec{u} + \nabla \vec{u}^T), \\ \boldsymbol{\sigma} &= \lambda \text{Tr}(\boldsymbol{\varepsilon}_{\text{el}}) \mathbf{I} + 2\mu \boldsymbol{\varepsilon}_{\text{el}},\end{aligned}\tag{4}$$

where the linear-elastic properties of the solid material are given by λ and μ , $\text{Tr}(\cdot)$ denotes the trace of a tensor, \mathbf{I} is the unit tensor. The molar volume expansion is given by θ . By this, the electrochemical model and the mechanical model are coupled as

$$\mu_{\text{el}} = \frac{\theta}{3} \text{Tr}(\boldsymbol{\sigma}) \Leftrightarrow \boldsymbol{\varepsilon}_{\text{ch}} = \frac{\theta}{3} c_s \mathbf{I},\tag{5}$$

where μ_{el} denotes the elastic part in the electro-chemical potential.

The electrolyte is assumed as an incompressible fluid with bulk modulus K .

Interface conditions

On the electrode-electrolyte interfaces, interface conditions are defined by the Butler-Volmer conditions as

$$i_{\text{se}} = i_0(c_s, c_e) \sinh\left(\frac{F}{2RT}\eta\right), \quad f_{\text{se}} = \frac{i_{\text{se}}}{F}, \quad \eta = \phi_s - \phi_e - \frac{\mu_s}{F},\tag{6}$$

Here, η is called the electro-chemical overpotential and μ_s is the chemical potential of the solid. The difference η of electro-chemical potentials on either side of the interface is only zero in the static thermodynamical equilibrium. The function i_0 is called the exchange current density, possibly defined as

$$i_0(c_s, c_e) = 2k \sqrt{c_e c_s \frac{c_{\text{max}}}{2}},\tag{7}$$

where k is the Butler-Volmer exchange coefficient and c_{\max} is the maximum solid lithium ion concentration. The electric current i_{se} is used to define Neumann boundary conditions for the Poisson equations of the electric potential while the concentration flux f_{se} is used to define Neumann boundary conditions for the diffusion equations of the lithium ion concentration. The Faraday constant F acts as a coupling factor. By the positive lithium ion charge, diffusion is coupled to the electric current. A fixed electric current is defined by the C-rate, usually specified in the unit per hour, i.e., $\frac{1}{3600s} = \frac{1}{h}$. C-rate 1 defines a charging current i_{in} such that it takes one hour to charge the battery cell from empty to full state of charge. For the diffusion equations and the elastic equations valid boundary conditions are considered. A discharged battery is considered for the numerical simulation test case.

2 Microstructure characterization

To give an example of application of the proposed method to realistic 3D data, in the present paper the microstructure of lithium-ion battery anodes is considered. A parametric stochastic 3D microstructure model has been developed and fitted to tomographic image data of the system of active particles in energy cell anodes in [2], see also [14] for power cell anodes and [8] for cathodes. Once calibrated to a given data set, stochastic microstructure models can be used to generate microstructures on the computer that are similar in a statistical sense to the data being modeled according to several morphological properties. Moreover, by systematic variation of model parameters it is possible to generate virtual, but realistic microstructures for materials that have not (yet) been manufactured in the laboratory. The combination of stochastic microstructure modeling with numerical simulations of functional properties allows us to identify preferable microstructures, a procedure called virtual materials testing.

The model proposed in [2] has been validated with respect to electrochemical properties using spatially resolved simulations in [3]. In the present paper, a comparison of mechanical properties computed for tomographic image data and for realizations of the calibrated model is performed.

The construction of the model is based on three main steps. To begin with, the sampling window is decomposed into a system of convex polytopes using a Laguerre tessellation, see Figure 1 (i). Later on, a particle will be placed in each polytope. However, to ensure complete connectivity of the system of particles, in the second step a connectivity graph is constructed, see the blue lines in Figure 1 (ii). This graph indicates which particles are supposed to be connected, i.e., if there is an edge of the graph between two polytopes, the corresponding particles will be forced to touch each other. In the third step, the particles themselves are modeled using spherical harmonic expansions of Gaussian random fields on the sphere. Thereby, the additional constraints that predefined points on the facets between those Laguerre polytopes where an edge of the connectivity graph is present are hit by the particles ensures that the particles touch each other as desired, see Figure 1 (iii). Then, the tessellation and connectivity graph are deleted, as they were only auxiliary tools for constructing the system of particles, see Figure 1 (iv). As a postprocessing step, a morphological closing is performed to mimic the effect of binder, see Figure 1 (v). A 3D

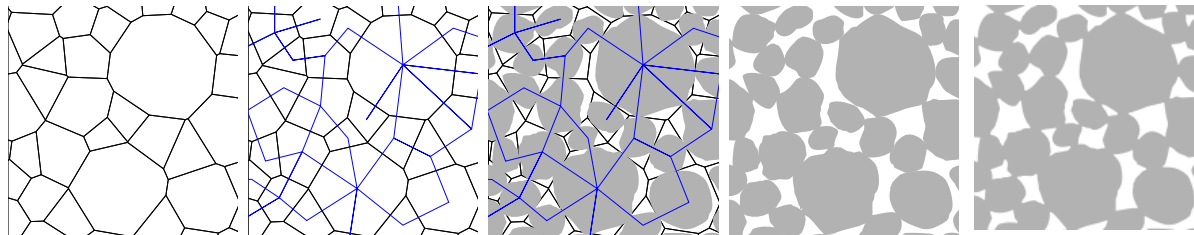


Figure 1: 2D sketch showing the individual steps of the stochastic microstructure model proposed in [2]. (i) Decomposition of the sampling window into convex polytopes. (ii) Construction of a connectivity graph. (iii) Modeling of particles according to the constraints given by the connectivity graph. (iv) The auxiliary tools are deleted. (v) A morphological closing is performed to mimic the effect of binder. Reprinted from [2], with permission from Elsevier.

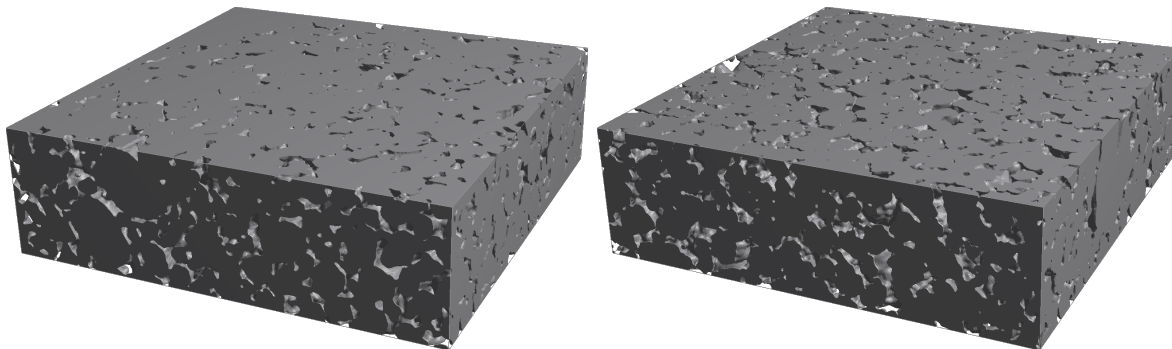


Figure 2: Left: CT image. Right: Simulated structure using the calibrated stochastic model.

comparison of tomographic image data and a corresponding model realization is shown in Figure 2.

3 Numerical methods

The governing equations of the electrochemical model are separated into six smaller initial-boundary-value-problems (IBVPs). The focus is on the coupling of those six different IBVPs in anode, cathode and electrolyte for both lithium ion concentration and electric potential. The coupling by the non-linear Butler-Volmer equations is solved using iteration. The convergence order of the domain decomposition algorithm is one.

Next the immersed interface method (IIM) is introduced for both the time-independent Poisson equation and the time-dependent diffusion equation. For the solution finite difference stencils and implicit Runge-Kutta schemes may be applied. Methods with convergence order two, four and six can be defined for the periodic Poisson equation and the periodic diffusion equation.

Assume that the diffusion equation is given on an arbitrary domain Λ . Then a discretization in time with an implicit Euler method with time step size τ and in space with a symmetric finite difference stencil with discretization width h results in the equation

$$(I_h + \tau \Delta_h)c_h = \check{c}_h, \quad (8)$$

where c_h and \check{c}_h denote the concentration field for the current and previous timestep, respectively, and I_h and Δ_h denote the discrete unit tensor and the discrete Laplacian operator, a finite difference stencil of second order. This equation is extended to include additional jump variables g_h on the boundary $\partial\Lambda$ that allow for an embedding of the equation onto a larger cuboid domain Ω ,

$$\begin{pmatrix} I_h + \tau\Delta_h & \Psi \\ D & I_h \end{pmatrix} \begin{pmatrix} c_h \\ g_h \end{pmatrix} = \begin{pmatrix} \check{c}_h \\ f_h \end{pmatrix}, \quad (9)$$

where f_h denotes arbitrary Neumann boundary conditions on $\partial\Lambda \subset \Omega$. The matrices Ψ and D are called projection matrix and differentiation matrix, respectively. In special cases they equal finite difference stencils and represent discretized delta distributions. The enlarged block system is then reduced by Schur's complement to

$$(I_h - D(I_h + \tau\Delta_h)^{-1}\Psi) = f_h - D(I_h + \tau\Delta_h)^{-1}\check{c}_h. \quad (10)$$

This allows for an efficient numerical solution as the number of variables is significantly reduced. Given a regular voxel mesh discretization with width h , the number of degrees of freedom inside Λ is in the order of $O(\frac{1}{h^3})$, while the number of degrees of freedom on the boundary domain $\partial\Lambda$ is in $O(\frac{1}{h^2})$. A second-order formulation for the immersed interface methods can be given.

The mechanical subproblem is solved and discretized on the same grid and linearized. The linear system is then solved with either a conjugate-gradient method for the linear-elastic problem or a Neumann fixed-point method if the non-linear plastification model is used. As a pre-conditioner, an operator representing a reference material with constant-coefficients is applied using Fast-Fourier methods [12].

4 Numerical examples

For validation of the method, a typical academic example as presented in other work [7, 11] is chosen. Figure 3 shows the lithium-ion concentration and corresponding stress invariants in an anode spherical particle with diameter 10 μm in radial direction during different states of charge. As the particle is spherical, no difference along tangential directions of the particle is observed and the properties only vary along the radial direction. While the Von-Mises stress maximum is situated in the outer shell of the particle, a local maximum of the hydrostatic stress is located in the center of the particle, compare to corresponding results in [13, 7, 6]. There, single particles without enwrapping electrolyte are discussed. Here, in the presented results, the increasing stress at the outer shell of the particle is due to the pressure of the enwrapping electrolyte, which is modeled as an incompressible fluid. Appropriate models for the electrolyte as well as periodic mechanical boundary conditions are open for discussion.

Figure 4 shows a comparison of the lithium-ion concentration and stress invariants in two different microstructures of anode material charged with C-rate 1 at 40% state of charge. In the top row, a tomographic image is depicted, while in the bottom row a realization of the calibrated stochastic microstructure model is shown. The electrode

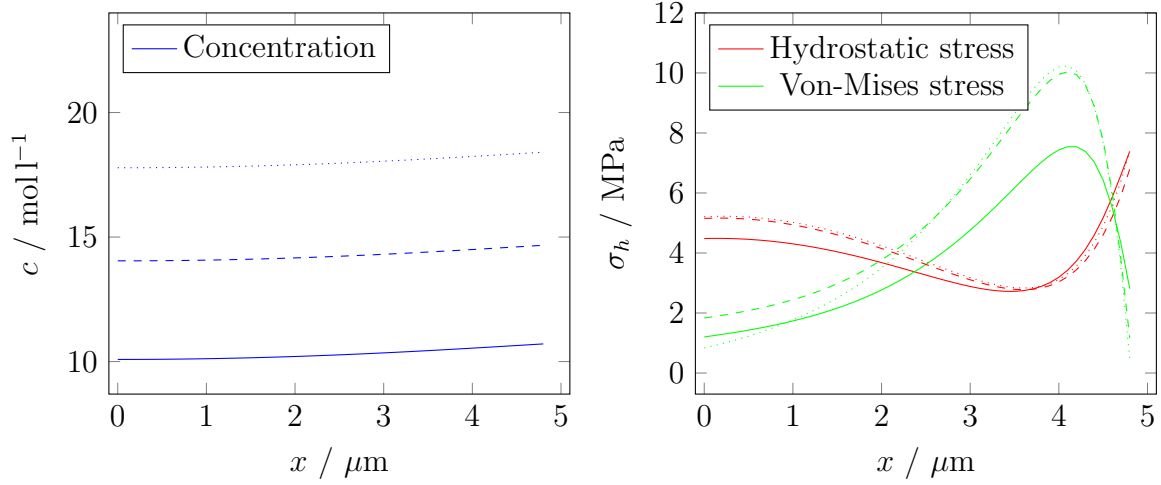


Figure 3: Radial-symmetric solution of (i) lithium-ion concentration and (ii) hydrostatic stress and von-Mises stress in a spherical particle for states of charge 40%, 55% (dashed) and 70% (dotted).

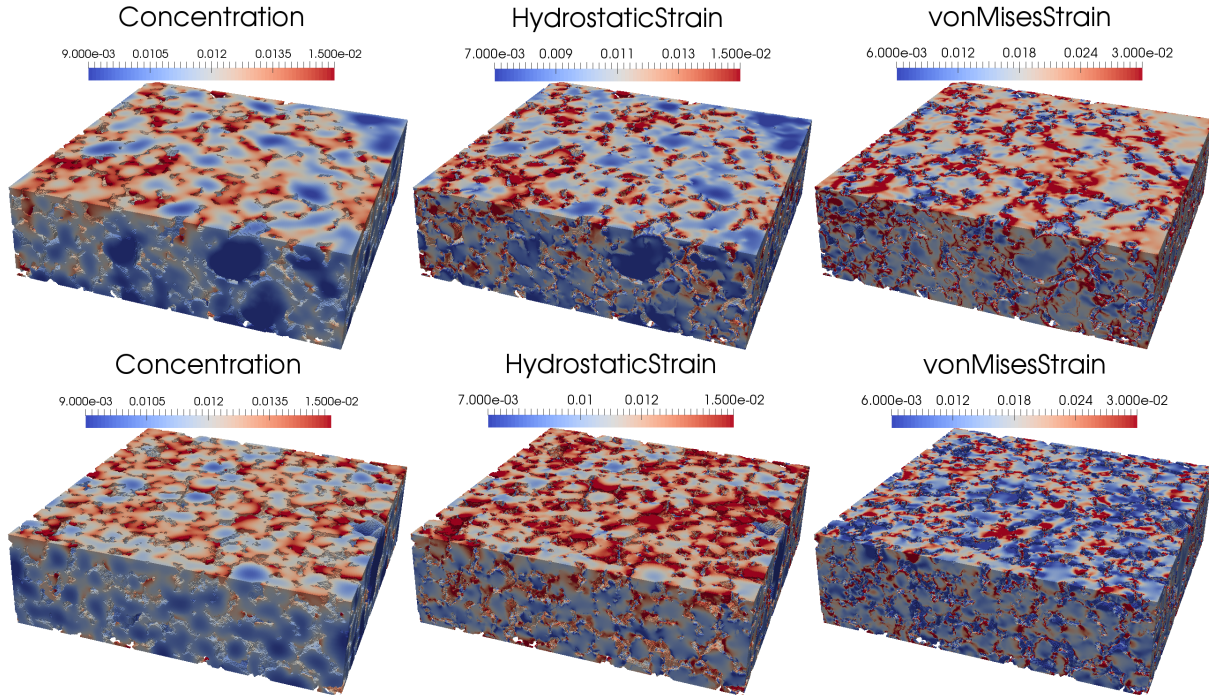


Figure 4: Full-field solution of lithium-ion concentration, hydrostatic stress and von-Mises stress in both tomographic (top) and simulated (bottom) microstructures.

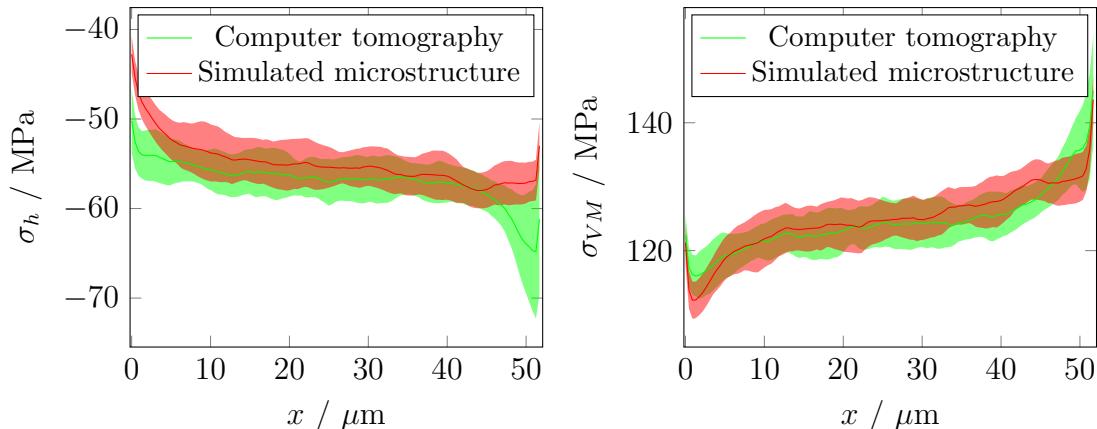


Figure 5: Comparison of the hydrostatic stress (left) and the von-Mises stress (right) for SOC=40% in the thickness direction. Plotted is the mean as well as ± 1 standard deviation.

structure is charged from top to bottom. Concentration gradients arising from uneven interface current densities can be seen. The inner center of larger particles remains empty. Maxima of hydrostatic stress occur together with maxima of the lithium-ion concentration. Maxima of the von-Mises stress occur mainly at particle boundaries.

For a more thorough analysis, a total of 22 cutouts of tomographic image data and 20 simulated model realizations of the same size were chosen. These 42 examples of anode microstructures were charged separately each with C-rate 1. Then the full-field solution for both stress invariants was averaged along the second and third dimension such that a spatial trend along the through-plane direction remains. Then for both, tomographic image data and model realizations, the results were averaged and the mean and standard deviation were calculated. Figure 5 shows the resulting curves and ± 1 standard deviation. While boundary effects can be seen in both stress invariants, the deviations between the computer tomography solution and the stochastically generated structures are within the standard deviations. This shows that, except for the boundary of the structure, mechanical properties are in good agreement between real and simulated data. The differences at the boundary can be attributed to the fact that the solid volume fraction is larger on the boundary than in the center for tomographic image data, while this effect is not reproduced in the stochastic microstructure model.

Conclusions

A micromodel coupling lithium-ion diffusion to the electric potential, Butler-Volmer interface currents and linear elasticity is applied. Mechanical stresses resulting from strains depending on the concentration are computed. Different microstructures are analyzed, which, e.g., allows for a comparison of mechanical properties between tomographic image data and simulated realizations of a stochastic microstructure model. Overall, a good agreement was found. Moreover, the approach allows us to investigate morphological advantages with respect to mechanical properties. Depending on material parameters the maximum C-rate and cycling effects can be evaluated. So far, the evaluation of maximum

stress invariants inside the battery electrode particles allowed only for rough qualitative prediction of time and point of failure. In the future, additional damage or fracture models will allow for a more precise prediction of the aging under realistic load cases. In combination with stochastic microstructure modeling, a broad spectrum of virtual, but realistic microstructures can be analyzed accordingly, and morphologies with preferable mechanical properties can be identified.

REFERENCES

- [1] L. Chen, F. Fan, L. Hong, J. Chen, Y. Z. Li, S. L. Zhang, T. Zhu, L. Q. Chen, *A phase-field model coupled with large elasto-plastic deformation: Application to lithiated silicon electrodes*. Journal of The Electrochemical Society. 161.11 (2014), F3164–F3172.
- [2] J. Feinauer, T. Brereton, A. Spetl, M. Weber, I. Manke, V. Schmidt, *Stochastic 3D modeling of the microstructure of lithium-ion battery anodes via Gaussian random fields on the sphere*. Computational Materials Science 109 (2015), 137–146.
- [3] S. Hein, J. Feinauer, D. Westhoff, I. Manke, V. Schmidt, A. Latz, *Stochastic microstructure modelling and electrochemical simulation of lithium-ion cell anodes in 3D*. Journal of Power Sources 336 (2016), 161–171.
- [4] T. Hofmann, R. Müller, H. Andrä, J. Zausch, *Numerical simulation of phase separation in cathode materials of lithium ion batteries*. International Journal of Solids and Structures, 100-1001 (2016), 456–469.
- [5] T. Hofmann, R. Müller, H. Andrä, *A fast immersed interface method for the Cahn-Hilliard equation with arbitrary boundary conditions in complex domains*. Computational Materials Science, 140 (2017), 22–31.
- [6] M. Huttin, M. Kamlah, *Phase-field modeling of stress generation in electrode particles of lithium ion batteries*. Applied Physics Letters 101.13 (2012) 133902
- [7] M. Klinsmann, D. Rosato, M. Kamlah, R. M. McMeeking, *Modeling crack growth during Li Extraction in storage particles using a fracture phase field approach*. Journal of the Electrochemical Society, 163.2 (2016), A102–A118.
- [8] K. Kuchler, D. Westhoff, J. Feinauer, T. Mitsch, I. Manke, V. Schmidt, *Stochastic model for the 3D microstructure of pristine and cyclically aged cathodes in Li-ion batteries*. Modelling and Simulation in Materials Science and Engineering, 26 (2018), 035005.
- [9] A. Latz, J. Zausch, *Thermodynamic consistent transport theory for Li-ion batteries*. Journal of Power Sources 196.6 (2011), 3296–3302.
- [10] R. J. LeVeque, Z. Li, *The Immersed Interface Method for Elliptic Equations with Discontinuous Coefficients and Singular Sources*. SIAM Journal on Numerical Analysis 31 (1994), 1019–1044.

- [11] V. Malavé, J. R. Berger, H. Zhu, R. J. Kee, *A computational model of the mechanical behavior within reconstructed Li_xCoO_2 Li-ion battery cathode particles*. *Electrochimica Acta*, 130 (2014), 707–717.
- [12] M. Schneider, F. Ospald, M. Kabel, *Computational homogenization of elasticity on a staggered grid*. *International Journal for Numerical Methods in Engineering*, 105.9 (2015), 693–720.
- [13] P. Stein, B. Xu, *3D Isogeometric Analysis of intercalation-induced stress in Li-ion battery electrode particles*. *Computer Methods in Applied Mechanics and Engineering*, 268 (2014), 225–244
- [14] D. Westhoff, J. Feinauer, K. Kuchler, T. Mitsch, I. Manke, S. Hein, A. Latz V. Schmidt, *Parametric stochastic 3D model for the microstructure of anodes in lithium-ion power cells*. *Computational Materials Science*, 126 (2017), 453–467.
- [15] X. Zhang, W. Shyy, A. M. Sastry, *Numerical Simulation of Intercalation-Induced Stress in Li-Ion Battery Electrode Particles*. *Journal of The Electrochemical Society* 154.10 (2007), A910–A9160.